

Deep autoencoder architecture for bridge damage assessment using responses from several vehicles

Muhammad Zohaib Sarwar^{*}, Daniel Cantero

Department of Structural Engineering, NTNU Norwegian University of Science and Technology, Trondheim 7491, Norway

ARTICLE INFO

Keyword:

Structural Health Monitoring
Damage detection
Indirect monitoring
Deep learning
Autoencoders
Convolutional neural network
Vehicle-bridge interaction

ABSTRACT

Vehicle-assisted monitoring is a promising alternative for rapid and low-cost bridge health monitoring compared to direct instrumentation of bridges. In recent years, centralized management systems for fleets of heavy vehicles have been adopted in transportation networks for logistics and other applications. These vehicles can be instrumented and easily integrated with the existing fleet management systems to provide information that can be used for bridge health monitoring. In this study, a numerical investigation is carried out to evaluate the feasibility of an indirect bridge monitoring system considering responses from several vehicles under operational conditions. The proposed method uses the vertical acceleration responses from a fleet of vehicles passing over a healthy bridge to train a deep autoencoder model (DAE) for bridge damage sensitive features. It is shown that the error in signal reconstruction from the trained DAE is sensitive to damage, when considering the distribution or results from several separate vehicle-crossing events. The bridge damage is quantified with a damage index based on the Kullback-Leibler divergence that evaluates the change in the distributions of the reconstruction errors. The performance of the proposed method is evaluated for two numerical scenarios of vehicle populations, for different damage cases including the effect of operational uncertainties (road profile, measurement noise, and variability in vehicle properties). The proposed method is also evaluated for more realistic multi-span continuous bridge for different damage cases in the presence of random traffic. The result show that the proposed method can detect damage under operational conditions and that it has the potential to become a new tool for cost-effective bridge health monitoring.

1. Introduction

The maintenance of ageing infrastructure is taking large parts of the total budget available to transport network owners. The continuously growing stock of bridges is getting old and many have exceeded their design service life. To ensure the safe operation of these bridges, monitoring and continuous assessment is essential. In recent years, structural health monitoring (SHM) strategies have evolved from manual inspection to sensors-based monitoring systems [1,2]. Sensor-based monitoring solutions require the direct installation of multiple sensing instruments on bridges and the analysis of the collected data [3]. The collected information from sensors is analysed through physics and/or data-driven techniques to extract useful features [4].

Early damage detection is one of the core objective in SHM and to that purpose many vibration-based methods have been proposed [4,5]. The measured vibration responses are analysed with some signal processing method to provide the information about the structure and

possible damage state. However, these methods generally require multiple sensors installed on the bridge, which increases installation and maintenance costs of the monitoring system. In addition, it is challenging to effectively utilize the large data sets generated daily for each bridge [6]. Because of these practical and economic considerations, the implementation of such systems is generally limited to a relatively small amount of long-span bridges [7].

As an alternative to traditional SHM methods, many studies have proposed indirect or 'Drive-by' methods. This idea utilizes the measured responses from a moving vehicle while traversing the bridge of interest. The method was initially proposed by Yang et al. [8] to identify the bridge's natural frequencies. This method is a low-cost alternative to traditional monitoring methods because it removes the necessity for individual instrumentation of each bridge. Over the past decade, researchers have investigated and provided many solutions for different damage detection levels using the indirect method [9]. These methods are broadly categorized into two main groups: (1) modal-based; (2) non-

^{*} Corresponding author.

E-mail addresses: muhammad.z.sarwar@ntnu.no (M.Z. Sarwar), daniel.cantero@ntnu.no (D. Cantero).

modal-based.

The modal-based indirect method identifies the bridge modal properties, which in turn can be used for damage detection [7,10]. Experimental validation of bridge frequency identification is done in [11] using instrumented trailer. Similarly, Yang et al. [12] and Zhu et al. [13] used empirical mode decomposition (EMD) and ensemble empirical mode decomposition (EEMD) for pre-processing the vehicle's acceleration response to extract higher mode frequencies of a bridge. O'Brien et al. [14] and Kildashti et al. [15] used the EMD and corresponding intrinsic mode functions (IMFs) to define a damage indicator. Modal-based indirect methods have been also used for mode shape identification, which allowed the detection and localisation of damage by analysing the mode shape curvature [16,17]. Yang et al. [18] proposed using the Hilbert amplitude of the acceleration response of passing vehicles to find bridge mode shapes. Likewise, Malekjafarian et al. [19] used the short-time frequency domain decomposition for bridge mode identification. Eshkevari et al. [20] proposed the novel pipeline methods together with EMD and structural identification using expectation maximization (STRIDEX) to identify mode shapes. Despite the advancements in the modal-based method, there are still critical challenges associated with it. Arguably, the main challenge is the need of low vehicle speeds in order to achieve sufficient resolution to accurately extract the modal parameters. Also, the performance of these methods is affected by the presence of the road profile and measurement noise.

In contrast, several other indirect methods did not directly extract modal parameters. These non-modal-based methods, which mainly rely on signal processing and machine learning, have been proven effective in detecting and localising damage [21–28]. For instance, Zhang et al. [27] proposed the estimation of contact-point response to detect damage. The vehicle-bridge contact point was estimated using acceleration measured on a vehicle. Then an indicator based on the Hilbert instantaneous amplitude was proposed for damage detection and localization. O'Brien et al. [21] effectively applied the moving force identification method for damage detection in a numerical study and verified it in an experimental investigation [29]. Both studies assume prior knowledge of the vehicle's dynamic properties (masses and suspension stiffness and viscous damping). Additionally, several authors have used wavelet transform in indirect methods. McGetrick and Kim [30] proposed a damage indicator based on the coefficients from the continuous wavelet transform (CWT), which was capable of identifying different crack levels on a bridge. Similarly, Hester and González [31] use CWT with the Mexican Hat basis for the detection of cracks on the bridge. Liderman et al. [32] applied signal processing and principle component analysis (PCA) to diagnose numerically simulated damage. Liu et al. [33] proposed a nonlinear dimensionality reduction method for damage diagnosis, studied it numerically for a single degree of freedom vehicle and verified it with laboratory experiments. Therefore, it is well acknowledged that these methods can perform well for damage detection and can be used to quantify the severity of the damage. However, their practical viability still requires significant physical insights for model and method selection.

Despite the reported progress in indirect health monitoring, several challenges and limitations still exist for its practical implementation. Bridge damage detection is a task that requires several vehicle passages and most of the 'Drive-by' methods generally use a single specialized vehicle. Thus, arguably the main challenge in this scenario is that it is practically impossible to have the same vehicle with the same properties over an extended period of time. In addition, operational and environmental conditions also directly affect the damage diagnosis process. To address these issues multiple frequent runs are an alternative approach for bridge monitoring. Miyamoto et al. [34] proposed the idea of using a fleet of public transport buses to monitor short and medium span bridges. A damage indicator was developed based on the average characteristic deflection curve. The authors suggested that heavy vehicle responses can be a better option for damage detection because of high flexural stiffness of short and medium-span bridges. Mei et al. [25] used

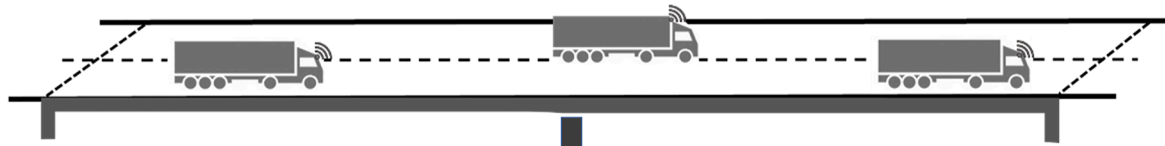
cepstrum analysis and PCA for damage detection from several vehicle-crossing events. Similarly, Malekjafarian et al. [26] and Locke et al. [35] proposed the idea of using artificial neural network (ANN) and deep learning respectively for damage detection using multiple vehicles measurement responses based on numerically generated vehicle-bridge interaction (VBI) data. In [26] the authors employed a two-stage approach using an ANN model and gaussian process (GP) to detect damage features from acceleration responses measured at the vehicles' axles. The combination of ANN and statistical analysis proved to be successful in the detection of damage even in the presence of surface roughness and measurement noise. Locke et al. [35] further explored this idea to only use a single deep learning model for feature extraction and damage diagnosis while considering operational and environmental affect. The main drawback was that it required labelled data of damaged cases, which is not possible in a real case scenario. The above-mentioned methods demonstrated that multiple vehicle responses analysed with different tools (signal processing, ANN and/or statistical analysis) can be successfully employed in indirect SHM. However, generally these studies are based on numerical simulations of simple vehicle models (mainly quarter-car). Furthermore, these studies consider only a small variation in vehicle properties and limited effect of road profile roughness.

On the other hand, recent developments in intelligent transportation systems has created the possibility to manage the information from multiple vehicles using a centralized system [36]. With progress in telemetric technology, the perspective of an on-board monitoring system for multiple vehicles managed via a centralized system opens new prospects for SHM. The multi-sensor (GPS, acceleration, speed, etc.) data from a fleet of vehicles can be remotely accessed regularly by system managers [37,38]. The big data that is collected from multiple vehicles can be further analysed and used for SHM. For big data analysis machine learning algorithms have proven to be a valuable tool to extract reliable information. Hinton and Salakhutdinov [39] introduced the idea of the deep learning (DL) model in machine learning to address the issue of gradient vanishing and convergence to local minima associated with shallow ANN architecture models. Since then deep neural networks have attracted attention in a wide range of applications, mainly in object recognition, speech recognition and natural language processing [40,41]. For SHM, DL models have been widely explored recently [42], where convolution neural networks (CNN) or recursive neural networks (RNN) are some of the DL algorithm types used. Abdeljaber et al. [43] proposed applying 1D CNN to extract structural damage features from the time histories of vibration responses. Similarly, Ni et al. [44] and Zhang et al. [45] used 1D CNN for data compression for anomaly detection in acceleration data for bridge health monitoring. Wang and Cha [46] and Shang et al. [47] used deep convolutional autoencoder to detect damage using directly measurements from the structure. For more details on recent advancements in vibration-based condition assessment, refer to [42,48], which provide a comprehensive review of DL and CNN applications in SHM.

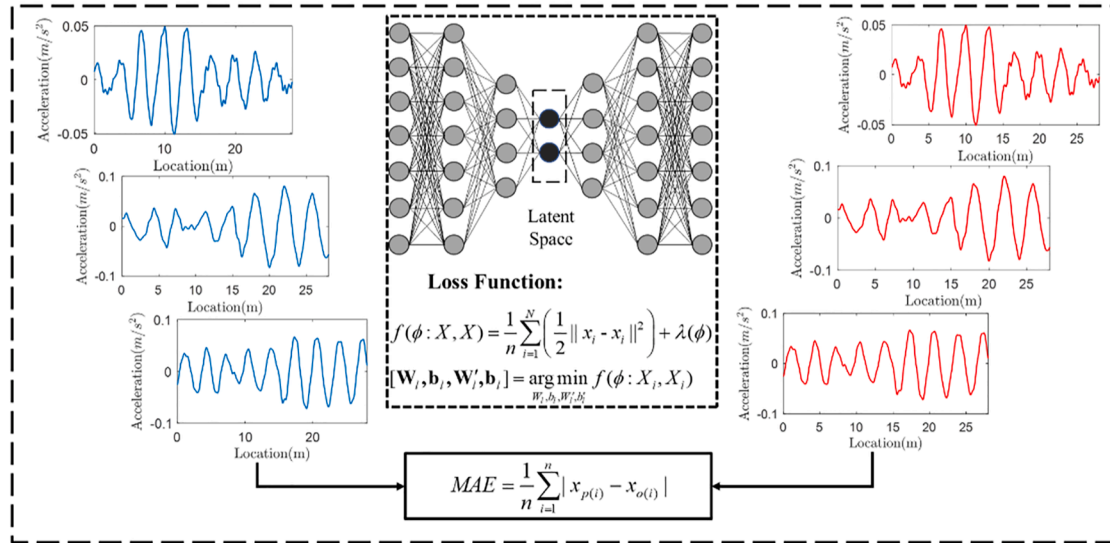
To address the challenges discussed earlier, we propose a bridge damage detection method considering the dynamic responses from a fleet of vehicles traversing the target bridge. The idea is explored numerically with a 5-axle truck model considering a range of vehicle properties and speeds, as well as, the presence of road profiles and measurement noise. An autoencoder based DL framework is trained to extract damage-sensitive features, where the inputs are the vehicles' vertical accelerations while traversing the bridge. Once the model is trained it is used to predict subsequent vehicle responses. The difference between model-based and actual vehicle responses is the prediction error. A damage index is proposed based on the distance between the distributions of prediction errors. The numerical study evaluates the performance of the proposed method for a range of different damage scenarios.

The remainder of the paper is organized as follows. Section 2 provides an overview of the proposed methodology, including the

Data collection



Autoencoder model



Damage indicator

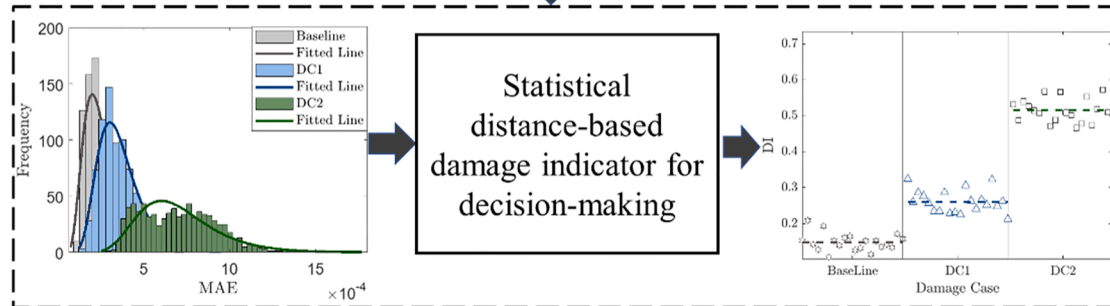


Fig. 1. Overview of the proposed framework.

architecture of the deep neural network model and damage index. Section 3 presents the vehicle-bridge interaction model and details about the training of the deep learning model. Section 4 evaluates the performance of deep learning model. Section 5 provides the numerical validation of the proposed damaged detection approach. Section 6 provides the validation of damage detection for multi-span continuous bridge model. Section 7 discusses the practical considerations for real life application of the proposed method

2. Proposed method

The framework proposed in this paper for damage detection is mainly divided into three phases. The first phase involves the collection of vehicle information and responses (speed and vertical acceleration) from a number of vehicle-crossing events. The collected data is then used to train a deep autoencoder for damage sensitive features in the second phase. The autoencoder architecture is developed using 1D CNN and Long short-term memory (LSTM) recurrent neural network. In the third phase, the trained model is used to compute the reconstruction error for testing data. The KL (Kullback-Leibler) divergence-based damage index is proposed to assess the severity of the damage. Fig. 1 shows a

schematic overview of the proposed framework. More details about the data collection, autoencoder, and damage index are discussed in subsequent sections.

2.1. Data collection

The proposed framework assumes that vehicle responses are measured using on-board systems, information that could be accessed remotely by a central fleet management system. Different sensor types could be used at different vehicle locations to measure a range of responses. However, due to their low cost and ease of installation, this study assumes that accelerometers are installed on each passing vehicle's tractor and trailer. Also, this study considers single-vehicle crossing events where the entry and exit times on the bridge are known.

2.2. Deep autoencoder (DAE)

Autoencoder is an unsupervised neural network model that is used for dimensionality reduction and feature extraction. The traditional architecture of autoencoder model consists of an encoder and a decoder module, each with a single hidden layer. The encoder module

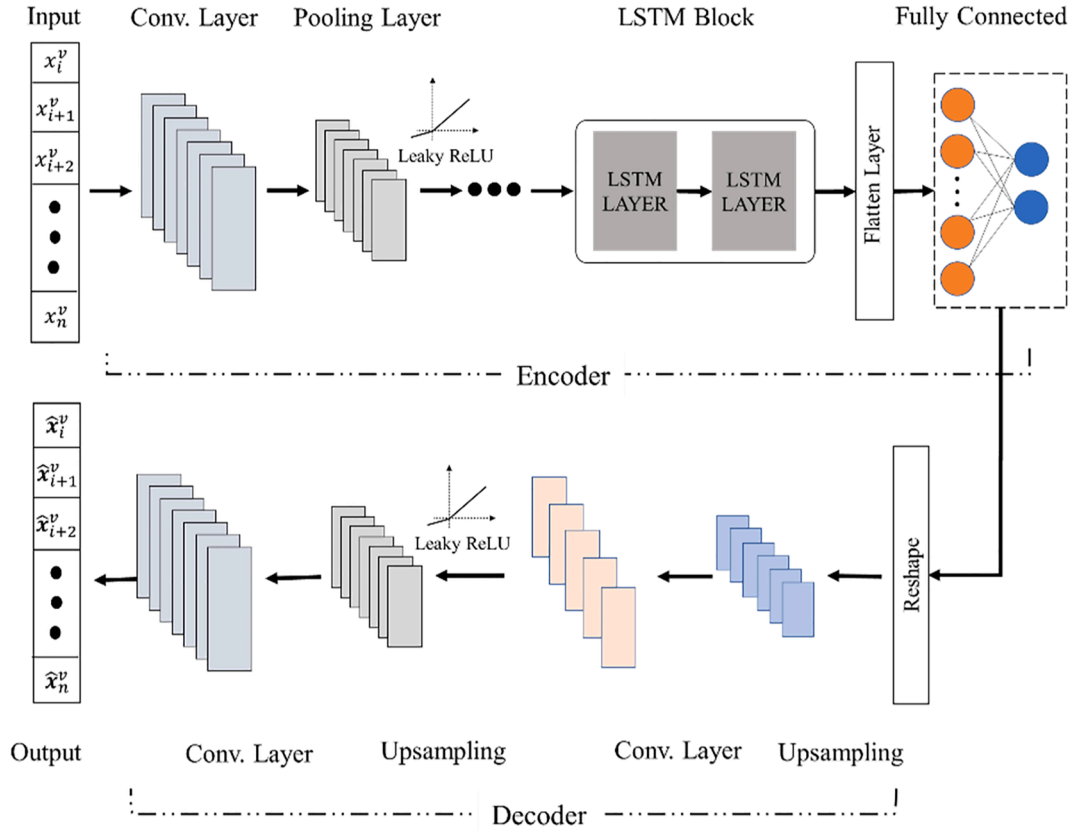


Fig. 2. Architecture of the proposed deep autoencoder model (DAE).

maps the input data x into arbitrary lower dimensional space h while the decoder modules reconstruct the original input using h as an output \hat{x} . The transfer function of each module is expressed as follows:

$$h = f(x) = \Phi(Wx + b) \quad (1)$$

$$\hat{x} = g(h) = \Phi'(W'h + b') \quad (2)$$

where W, W' and b, b' are the weight matrices and bias vectors for encoder and decoder modules, while Φ, Φ' are the activation functions of encoder and decoder, which are usually the nonlinear functions *sigmoid* or *hyperbolic tangent*. The autoencoder optimizes the learning parameters W, W', b, b' using mean squared error as the loss function \mathcal{L} between input and its reconstruction at the decoder's output.

In comparison to traditional autoencoders, deep autoencoders (DAE) contain more than one hidden layer (depending on the input data's complexity) in the encoder and the decoder. The DAE model allows for the effective feature extraction through hierarchical nonlinear mapping via multiple hidden layers, resulting in a significant reduction of training dataset [46]. For a DAE model, the loss function can be expressed for an unlabelled dataset $X = [x_1, x_2, x_3, \dots, x_n]$ as follows:

$$\mathcal{L} = f(\phi : X, X) = \frac{1}{n} \sum_{i=1}^n \left(\frac{1}{2} \|\hat{x}_i - x_i\|^2 \right) + \lambda(\phi) \quad (3)$$

$$\begin{aligned} [W_l, b_l, W'_l, b'_l] &= \underset{W_l, b_l, W'_l, b'_l}{\operatorname{argmin}} f(\phi : X, X); \\ l &= 1, 2, 3, \dots \end{aligned} \quad (4)$$

Where subscript l is the number of hidden layers and λ is a regularization factor imposed at the weights of the specific layer to prevent overfitting.

2.2.1. Network architecture for DAE

Autoencoders have been used in literature, among other

applications, for feature extraction and dimensionality reduction [49,50]. In the proposed framework, these functionalities are utilised to learn the compressed feature representation of multiple vehicles' acceleration responses, which can further be used for robust damage detection.

For feature extraction from time-series, recurrent neural network (RNN) and 1D convolutional neural network (1D CNN) are widely used. RNN is specifically designed for sequential data to extract and augment the time-dependent features. However, according to the existing investigations, it is difficult to train RNN for long term sequences because of gradient vanishing during backpropagation [51]. To address this Long short-term memory (LSTM) is introduced [52]. LSTM is explicitly designed to avoid the long-term dependency problem because of its internal gates-like architecture that can be used to control the flow of information. LSTM has a threshold-based mechanism to fuse similar information and filter out redundant information. More details regarding LSTMs can be found in [52].

A CNN usually consists of a convolutional layer, pooling layer, and activation function. In the convolutional layer, the convolutional operations are performed on the input by different convolutional filters, which essentially perform cross-correlation on multiple local regions of the input to extract low-level features from the raw response. The pooling layer aggregates the information from all local regions and downsamples the overall feature space. The pooling layer makes the learned feature robust and reduces the model's number of parameters, resulting in a computationally efficient model. The activation function is applied for nonlinear transformation in each layer.

DAE architecture is developed as shown in Fig. 2 to extract the compact hidden representation of the training dataset. The model can reconstruct the input data with high accuracy and is mostly sensitive to damage information. The hidden layers of the encoder have two levels. The first level includes multiple convolutional blocks, where each extract multiple local features from the input data and reduces the

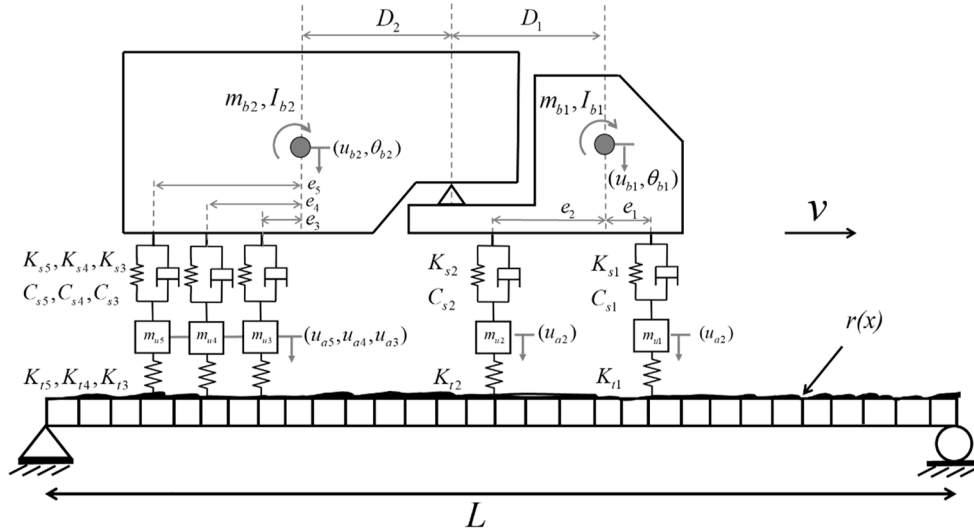


Fig. 3. Vehicle-bridge interaction model.

number of parameters by pooling layers. Here, the Leaky-ReLU activation function is used. In this first level, the time-series response is reduced to a more compact representation of the most relevant features. The extracted features using convolutional blocks are strongly dependent upon each other. However, 1-D CNN did not able produce smooth and compact latent representation that can be applied for reconstruction of the original response. For a robust latent representation, learning feature's temporal dependencies are crucial. A fully connected layer is normally used to simply combine the feature with its adjusted weight. However, in this case for smooth latent representation, the first level feature map is fed into a second-level LSTM layers for retaining the temporal dependencies of similar features which would further be used for extracting smooth latent space. Then the last LSTM layer is flattened and mapped to the bottleneck layer to obtain a fixed latent space representation. For the decoder, each convolutional block is comprised of deconvolutional layers followed by up-sampling and nonlinear activation function Leaky-ReLU. The proposed architecture optimization of weight and bias parameters is done by an end-to-end method, in contrast to stepwise training of hidden layers, and staking of pre-trained layers for final fine-tuning.

2.3. Damage index (DI)

For damage detection and severity evaluation, the reconstruction loss is evaluated by the mean absolute error (MAE) using Eq. (5). The MAE calculates for each vehicle, the difference between the measured response and the reconstructed response estimated by the trained DAE model.

$$MAE = \frac{1}{n} \sum_{i=1}^n |\hat{x}(t_i) - x(t_i)| \quad (5)$$

where $\hat{x}(t_i)$ and $x(t_i)$ are the reconstructed and measured responses respectively at sample i for a total of n samples.

When considering a fleet of vehicles, the MAE error significantly varies between crossing events because of the different vehicle properties and speed. However, batches of these events result in distributions of MAE values that can be used to differentiate a healthy bridge (baseline) from a damaged one. It is possible to assess the bridge condition by evaluating the difference between MAE distributions from different batches. In this study, KL divergence is computed to quantify how different two distributions are [53]. The KL divergence is the method that comes from information theory and measures the information loss when a probability distribution p is used to approximate a distribution q .

The general form of KL divergence is expressed as follows:

$$D_{KL}(p||q) = \int_x p \log \frac{dp}{dq} \quad (6)$$

In this paper the MAE distributions are assumed to follow the log-normal distribution for each batch of vehicles crossing the bridge. These distributions are defined in terms of their corresponding mean μ and standard deviation σ for the baseline condition ($p_0 = \log N(x|\mu_0, \sigma_0)$) and for an unknown condition ($q_1 = \log N(x|\mu_1, \sigma_1)$). By using the probability density functions definitions in Eq. (6) the KL divergence between two distributions can be written as:

$$D_{KL}(p_0||q_1) = \ln \left[\frac{\sigma_1}{\sigma_0} \right] + \frac{1}{2\sigma_1^2} [(\sigma_1^2 - \sigma_0^2) + (\mu_1 - \mu_0)^2] \quad (7)$$

One can see in Eq. (7) that the relationship between the distributions and KL divergence is exponential with a range of $[0, \infty]$. To obtain a robust damage index (DI) the expression is transformed into a linearized relationship as Eq. (8) as proposed in [54]. From Eq. (8) it is clear that DI value depends upon the batch size of vehicles. If sufficient amount of vehicle-crossing data is available, this DI could be used for damage detection. This would be later illustrated with numerical results in Section 5.

$$DI = \ln[D_{KL}(p_0||q_1) + e] \quad (8)$$

where e is Euler number.

3. Numerical modelling

This section presents the numerical model that simulates the responses of a vehicle-bridge interaction system with road profile. The numerical model would be used to generate dataset for training and evaluation of DAE. This section also discusses the configuration and hyperparameters for DAE training used in this study.

3.1. Vehicle-bridge interaction model

Fig. 3 shows the vehicle-bridge system used for numerical simulations. The coupled system is modelled as a simply supported beam crossed by a 5-axle truck.

3.1.1. Vehicle model

The vehicle model consists of an articulated tractor-trailer configuration with two and three axles respectively. Fig. 3 shows that the tractor

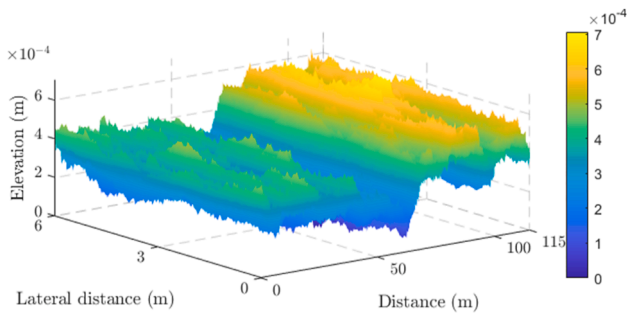


Fig. 4. Road profile of class A (according to ISO 8608).

and trailer are represented as rigid bodies, whereas the axles are modelled as lumped masses. These bodies are interconnected with spring and dashpot systems representing the suspensions. The axle tyre is modelled as a single spring connecting the axle mass and road profile. The vehicle model has a total of 8 independent degrees of freedom (DOF's): vertical displacements of five axles ($u_{a,i}$), tractor's vertical displacement (u_{b1}) and pitch rotation (θ_{b1}), and pitch rotation (θ_{b2}) of the trailer. The trailer's vertical displacement (u_{b2}) can be expressed in terms of the other DOFs by the geometric relation given in Eq. (9) arising from the articulation between tractor and trailer.

$$u_{b2} = u_{b1} + D_1\theta_{b1} + D_2\theta_{b2} \quad (9)$$

The equation of motion of the vehicle can be represented by:

$$M_v\ddot{u}_v + C_v\dot{u}_v + K_v u_v = f_v \quad (10)$$

where M_v , C_v , and K_v are the mass, damping and stiffness matrices of the vehicle respectively. The u_v vector contains the displacements of all DOFs and f_v is the external force applied to the vehicle system. The extended formulation can be found in [55]. The vehicle model assumes constant speed for each run. Table A1 in appendix provides the vehicle parameters adopted for the numerical studies. The values of the vehicles' parameters are based on European 5-axle trucks, which are adopted from [56–58]. Reference [58] also provides the parameters for distributions (mean, standard deviation, minimum and maximum) that are the basis for generation of batch of vehicles used for Monte Carlo simulations.

3.1.2. Bridge and road profile

The bridge is modelled as a simply supported beam of 15m span length. Its section and material properties are: second moment of area $I = 0.5273 \text{ m}^4$, modulus of elasticity $E = 3.5 \times 10^{10} \text{ N/m}^2$, and mass per unit length $\rho = 28125 \text{ kg/m}$, deemed to represent a generic reinforced concrete highway bridge. A 2% damping is considered for all modes. The finite element model is discretised into 30 elements (each element 0.5 m length). The equation of motion of the bridge is described as follows:

$$M_b\ddot{u}_b + C_b\dot{u}_b + K_b u_b = f_b \quad (11)$$

where M_b , C_b , and K_b are the global mass, damping and stiffness matrices of the bridge respectively and u_b is the vector of nodal displacements.

A road profile is also added to the bridge model. A 6 m wide carpet road profile of ISO class 'A' is generated as shown in Fig. 4. A 100 m approach distance is considered before entering the bridge to allow that traversing vehicles reach dynamic equilibrium. The transverse vehicle position on the road profile is randomly varied for each run following a normal distribution. A moving average filter of 0.24 m width is applied to the profile to represent the actual contact of a truck tyre [59]

3.1.3. Vehicle-bridge interaction:

The response of a vehicle traversing a bridge is characterised by the dynamic interaction between both systems. This vehicle-bridge inter-

action is achieved by coupling the equations of motion of vehicle Eq. (10) and bridge Eq. (11). The final system of coupled equations of motions can be expressed as:

$$M_g\ddot{u}_g + C_g\dot{u}_g + K_g u_g = f_g \quad (12)$$

where M_g , C_g , and K_g are the time-varying system mass, damping and stiffness matrices respectively and u is the vector of combined bridge and vehicle displacements. $u_g = \{u_b, u_v\}$. The vector f_g contains the external forces applied to the coupled system [55]. To solve the coupled system, the equation of motions are integrated using Newmark- β scheme and solved iteratively to obtain the system responses, which has been implemented in MATLAB. More details of the coupling procedure and numerical solution can be found in [55,60].

3.2. Data generation and pre-processing

Numerical evaluation of the proposed damage detection method is performed using simulated data generated by solving the vehicle-bridge interaction system presented in Section 3.1. In this study, two different scenarios are considered based on the degree of variation in vehicle properties.

1. Scenario-1: The dataset is generated assuming that a fleet of similar vehicles is traversing the bridge. In this case, the variation in vehicle properties is considered in such a way that their standard deviation is small, while the geometry of the vehicles is identical. Variation in vehicle masses and suspension properties is applied to account for normal fluctuations in payload and to account for the inherent uncertainty of the reported vehicle properties.
2. Scenario-2: This data represents a more generic scenario where the responses of different 5-axle trucks is considered. Compared to Scenario-1, the dataset is generated by randomly varying the vehicle properties with a larger standard deviation, while at the same time introducing also random variations in vehicle geometry, rendering different vehicles for each event.

The particular vehicle properties and the statistical variability of the parameters (i.e. maximum, minimum, and standard deviation) for both scenarios are presented in Table A1 in the appendix. For both datasets, the vehicle properties are randomly sampled based on the given statistical variation within a Monte Carlo simulation. For each scenario, a batch of 1000 vehicle events are created. Each dataset contains the vehicle's speed (v) and the vertical acceleration response from tractor (\ddot{u}_{b1}) and trailer (\ddot{u}_{b2}) with a sampling frequency of 500 Hz. The length of these signals is not uniform across the events in the datasets because of the varying vehicle's speed. For DAE input, the acceleration signals of each event are resampled into the spatial domain by multiplying signal in time by the vehicle's speed. Therefore, for each vehicle crossing the bridge of 15 m, 1500 samples are recorded. Therefore, the size of a dataset X , for either tractor (\ddot{u}_{b1}) or trailer (\ddot{u}_{b2}), is 1000×1500 . Each dataset is normalized using Eq. (13) for better reconstruction performance of DAE[47].

$$X_n = \frac{X - \mu_X}{\sigma_X} \quad (13)$$

where X_n is the normalized dataset, while μ_X and σ_X is the mean and standard deviation of the original data set X .

3.3. Configuration of DAE

The architecture of DAE is designed by using TensorFlow modules, and the implementation code is developed using python 3.7. The configuration of the autoencoder model was selected based on lowest reconstruction loss after an extensive trial and error process. The detail of different model configurations and parameters used in trial and error

Table 1
Different network architectures and hyper-parameters used for model selection.

Architecture	Latent size	Activation function	L_2 regularization
conv.-latent-conv. [4,6,8]-1- {4,6,8}	{8,16,32,64}	{tanh, ReLU, leaky-ReLU}	$\{10^{-2}, 10^{-4}, 10^{-6}\}$
conv.-LSTM-latent-conv. [4,6,8]-{1,2,3}-1- {4,6,8}	{8,16,32,64}	{tanh, ReLU, leaky-ReLU}	$\{10^{-2}, 10^{-4}, 10^{-6}\}$

*conv: convolutional block, LSTM: Long short-term memory layers.

Table 2
Architecture of proposed deep autoencoder.

Layers	Output shape	Kernel size	Activation
Encoder			
Input	(1500 × 1)	–	–
Conv_1D	(1500 × 256)	1 × 7	Leaky-ReLU
Max-pooling	(500 × 256)	1 × 7	–
Conv_1D	(500 × 128)	1 × 5	Leaky-ReLU
Max-pooling	(250 × 128)	1 × 5	–
Conv_1D	(125 × 64)	1 × 3	Leaky-ReLU
Max-pooling	(125 × 64)	1 × 3	–
Conv_1D	(125 × 32)	1 × 3	Leaky-ReLU
LSTM	(125 × 32)	–	Leaky-ReLU
LSTM	(125 × 32)	–	Leaky-ReLU
Flattened	(2000)	–	–
Fully connected	(16)	–	Leaky-ReLU
Decoder			
Fully connected	(4000)	–	Leaky-ReLU
Reshape	(125 × 32)	–	–
Conv_1D	(125 × 64)	1 × 3	Leaky-ReLU
Up-sampling	(250 × 64)	1 × 3	–
Conv_1D	(250 × 128)	1 × 3	Leaky-ReLU
Up-sampling	(500 × 128)	1 × 3	–
Conv_1D	(500 × 256)	1 × 3	Leaky-ReLU
Up-sampling	(1500 × 256)	1 × 3	–
Output	(1500 × 1)	–	Linear

*Conv_1D: 1-Dimensional convolutional layer, Leaky ReLU: Leaky-Retified linear unit, LSTM: Long short-term memory

process is summarized in Table 1. The final architecture's encoder module includes an input layer, four convolutional blocks, two LSTM layers, and fully connected layers. Each convolutional block has a 1D convolutional layer and a max-pooling layer followed by Leaky-ReLU as an activation function. For the decoder module, the same number of convolutional blocks is used as in encoder but in the reverse direction. In the decoder module, a max-pooling layer is replaced with up-sampling layer and at the output layer linear activation function is used. For robust model performance and to avoid overfitting, a regularization term is used as an additional hyperparameter. The regularization term applies penalties on weight parameters of the layers. In the proposed model, L_2 regularization is applied at the bottleneck layer with the value of 1×10^{-4} . The detailed architecture of the proposed DAE with different hyperparameters (activation function, filters and kernel size) is

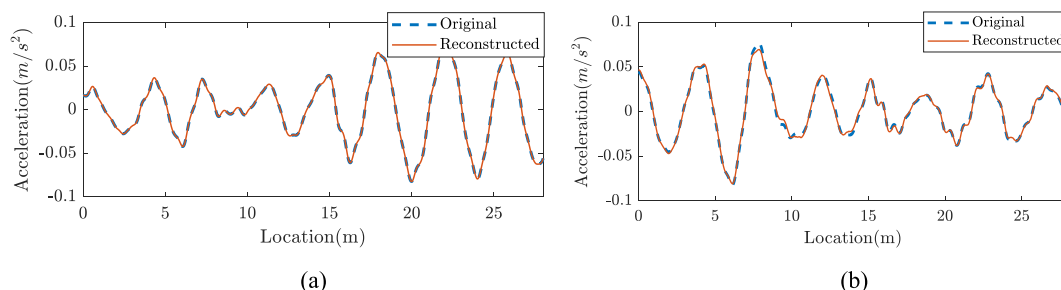


Fig. 5. Comparison of original and reconstructed vertical accelerations of two separate events for: (a) healthy and (b) damaged case.

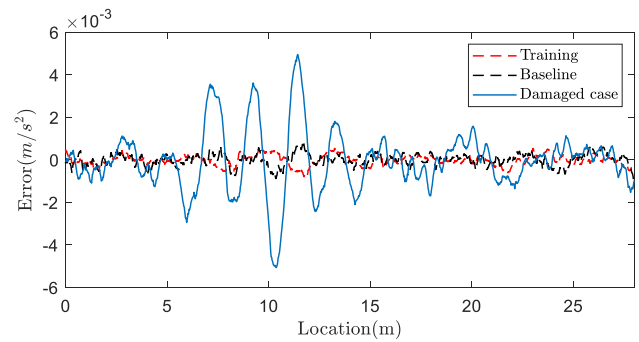


Fig. 6. Comparison of the difference between measured and reconstructed signals for three different vehicle-crossing events.

shown in Table 2. For evaluation of proposed method in subsequent sections same hyperparameters would be used for all scenarios.

The learning and decay rates are set to 0.001 and 0.0001 respectively for model optimization and training, adaptive moment estimation (Adam) with a batch size of 64 samples is considered. For efficient training, early stopping criteria is added to the network, which stops the training when the model achieves the loss criteria of 1×10^{-6} or 1500 epochs. All models training and numerical computations are performed on a standard PC with Intel Core i9-10900 K CPUs with 64 GB RAM and NVIDIA GTX 2080Ti graphic card.

4. Damage detection using DAE

This section evaluates the DAE for damage detection using Scenario-1, in which the crossing event correspond to a fleet of similar vehicles as discussed in Section 3.2. For this demonstration, the DAE model is trained with the acceleration responses from the tractor of the vehicles (\ddot{u}_{b1}). For training, the dataset is divided into 700 and 300 vehicle-crossing events for training and validation respectively. After training, the model achieves mean squared errors of 1.2908×10^{-6} and 1.2119×10^{-6} for training and validation data. The total training time was 1 h and 16 min. To demonstrate how the trained model can be used for damage detection, seven new datasets with different damage severities are generated for Scenario-1, in which the damage is modelled as a stiffness reduction of a single beam element. The details for the different damage cases (DC) are:

- Baseline: Dataset with no damage
- DC1: Dataset with 5% damage at midspan
- DC2: Dataset with 10% damage at midspan
- DC3: Dataset with 15% damage at midspan
- DC4: Dataset with 20% damage at midspan
- DC5: Dataset with 25% damage at midspan
- DC6: Dataset with 30% damage at midspan

To visualize the model's reconstruction performance, two random cases are illustrated for the baseline data (undamaged bridge) and

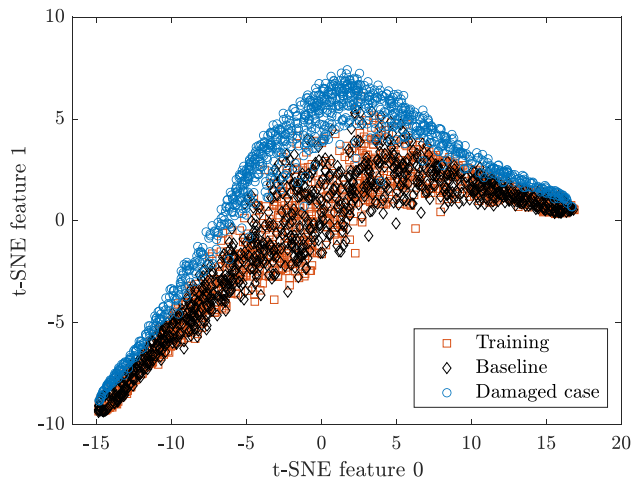


Fig. 7. Feature space visualization using t-SNE on the encoder output.

damage case (DC4). Fig. 5 shows the measured and predicted signals for two particular vehicle responses from different datasets. The trained DAE model is able to reconstruct the response for the healthy bridge case (Fig. 5(a)) with great accuracy, whereas for the damaged case (Fig. 5(b)) the match between measured and reconstructed signals is somewhat different. The proposed method exploits precisely this difference to detect damage. This reconstruction error shows large fluctuations between individual events but remains approximately constant when larger populations of events are analysed statistically.

To further quantify the loss in signal reconstruction, three particular vehicle-crossing events are investigated. The measured acceleration responses are compared to DAE’s reconstructed response in Fig. 6 that shows the difference between both. The errors for vehicles from the training dataset and baseline are very small and almost the same, while for a damaged case event, the model could not reconstruct the response with the same accuracy. The reason for the higher reconstruction loss is due to the damage in the bridge. Then, the dynamic behaviour of the bridge changes, which leads to inaccuracies in vehicle response reconstruction. Because the DAE is trained only for the healthy condition, the model cannot reconstruct the response accurately when data from a

damaged case is used.

The DAE model generalises the feature space into a continuous domain. This capability makes it possible to correctly predict the responses of events with different vehicle properties and travelling at different speeds, while at the same time distinguish changing bridge conditions. This is achieved because the encoder module in the DAE compresses the input data and transforms it into a latent space that generalises the feature space. To visualise this capability of the DAE model, the t-Distributed Stochastic Neighbour Embedding (t-SNE) is applied, which is used to compare high-dimensional datasets [61]. Fig. 7 shows a two-dimensional visualization of the feature space for the input data from three datasets (training, baseline, DC4). This confirms that the DAE model produces distinctive clusters for events with different damage conditions.

The studied example shows that it is possible to distinguish the structural condition by evaluating the reconstruction error for batches of events. To further illustrate this idea, Fig. 8 shows the histogram of the reconstruction errors in terms of MAE (Eq. (5)). The figure directly compares the distribution of errors of the baseline dataset with the different damage cases considered in this study (DC1 to DC6). The results show that as the damage increases, the mean absolute error distribution changes compared to the baseline. In the proposed method, this variation in the statistical distribution of different bridge conditions is exploited for damage detection and severity quantification.

In order to quantify the differences between batches of events, log-normal distributions are fitted to the histograms of mean absolute error. As shown in Fig. 8 the distribution of MAE is always positive, is skewed to the right and has a long tail because of outliers. The log-normal distribution has similar characteristics, namely a lower bound of zero and a positive skewness. Thus the log-normal distribution is deemed suitable for representation of the distribution of MAE. The statistical parameters of those fits are then used to define the damage index discussed in Section 2.3. Fig. 9 shows the fitted distributions to the results in Fig. 8. Each distribution has distinct statistical parameters (μ , σ) that are then used to compute the corresponding DI following Eq. (8).

5. Performance of damage detection method

This section evaluates the performance of the proposed damage detection method using vehicle responses for the two different scenarios

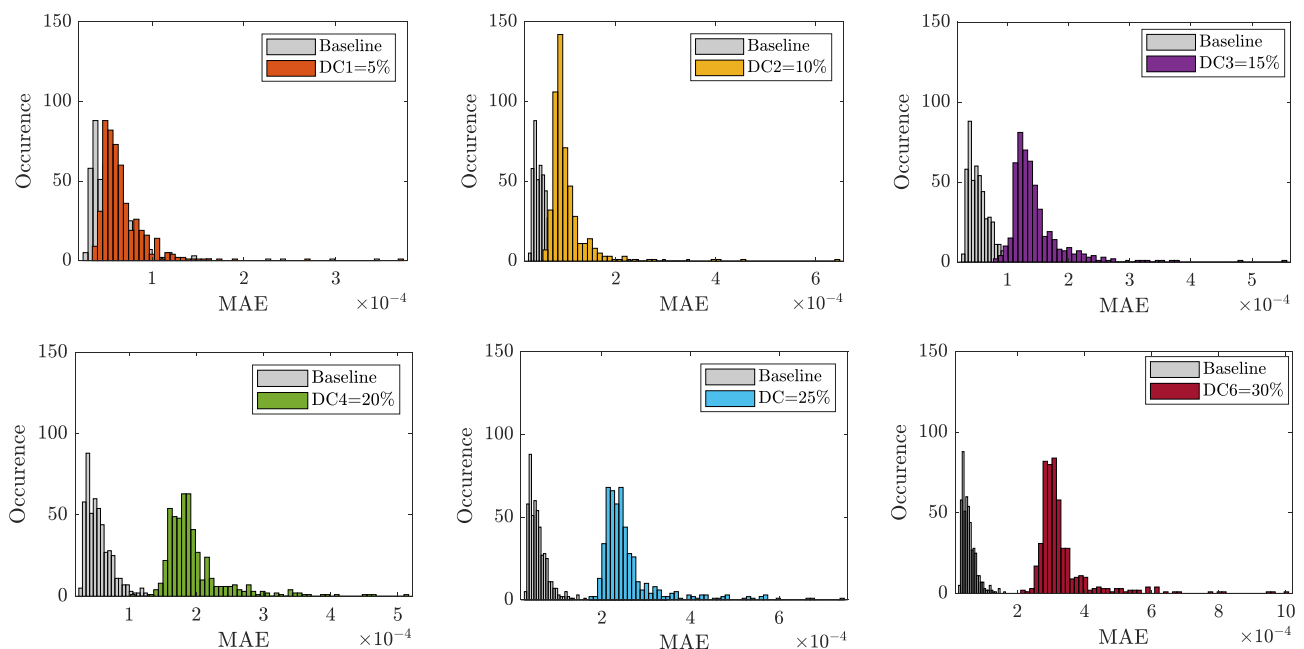


Fig. 8. Histogram of mean absolute error for batches of events for different bridge damage cases.

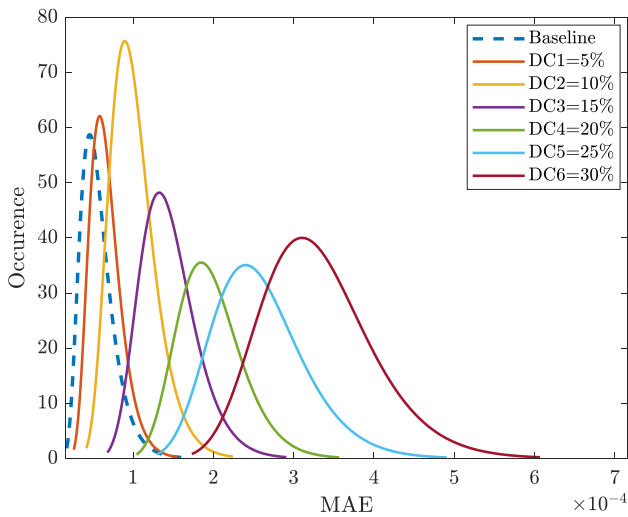


Fig. 9. Comparison of log-normal distributions of reconstruction loss for different damage cases.

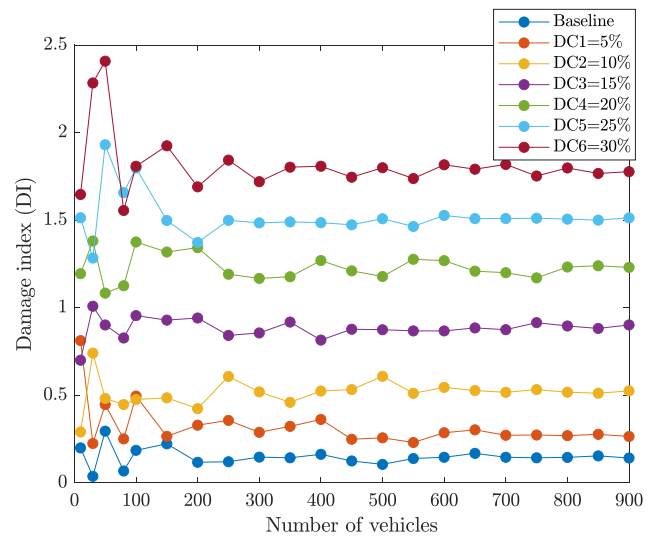


Fig. 11. Influence of batch size (number of vehicle-crossing events) in the calculation of the damage index.

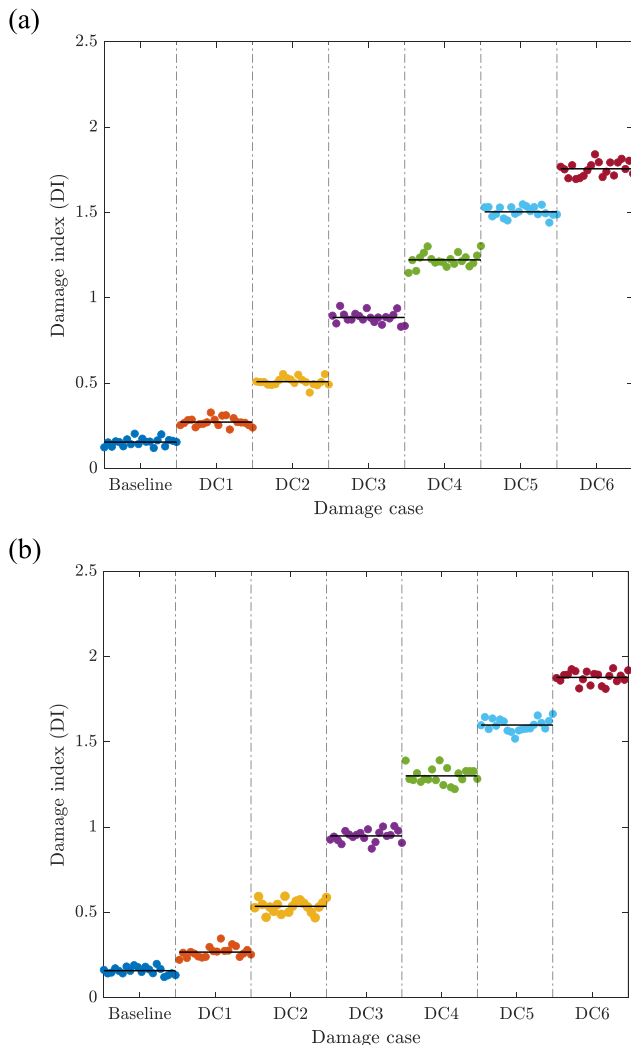


Fig. 10. Evolution of daily damage index (300 events/day) during progressive bridge condition change (every 20 days), for Scenario-1. Solid line indicates 20-day average value, using signals from: (a) tractor response (b) trailer response.

presented in Section 3.2. The analysis studies the sensitivity of the proposed damage index to damage severity and location. In addition, this section explores the influence of number of vehicles, their speeds and effect of measurement noise.

5.1. Damage detection for Scenario-1

This section illustrates how damage detection can be performed by using vehicle responses from a fleet of similar vehicles (Scenario-1) when there is a progressive bridge deterioration. This analysis assumes that for every given day, 300 vehicle-crossing events are available. The condition of the bridge is changed with increases of 5% damage severity every 20 days, starting from a perfectly healthy beam (baseline) until a 30% stiffness reduction at midspan (DC6). For comparison, this scenario is studied for acceleration responses from the tractor (\ddot{u}_{b1}) and the trailer (\ddot{u}_{b2}). Two separate DAE models are trained with acceleration responses from both locations on the vehicles.

Fig. 10 shows the damage index (DI) calculated using Eq. (8) for the discussed scenario. The DI values are distinctively different for different bridge conditions. In the case of the baseline, the magnitude of DI is small and close to zero. As the severity of the damage increases DI grows proportionally. The operational conditions and varying vehicle properties affect the magnitude of DI, which result in daily variations. However, for any given bridge condition the average value of the DI remains constant. The sensitivity of the index to the damage severity is clear, which allows the identification of damage even considering the daily dispersion in results. Therefore, it is evident that the proposed method can successfully be used to monitor the evolution in time of the condition of a bridge.

Fig. 10 also allows for a direct comparison of the damage detection method using signals from different locations in the vehicles. While the results in Fig. 10(a) come from the analysis of the vertical accelerations in the tractors, Fig. 10(b) shows the same analysis but based on the signals recorded on the trailers. Both sources of vehicle responses yield similar results in terms of sensitivity and variability of the DI. Therefore, in subsequent studies in this section only the tractor response (\ddot{u}_{b1}) will be considered.

5.1.1. Influence of the number of vehicles

The robustness and accuracy of the proposed method depends on the number of vehicles considered for a given batch of events. The damage index (Eq. (8)) directly relates to the probability distribution of the reconstruction error (MAE). Errors for individual events usually

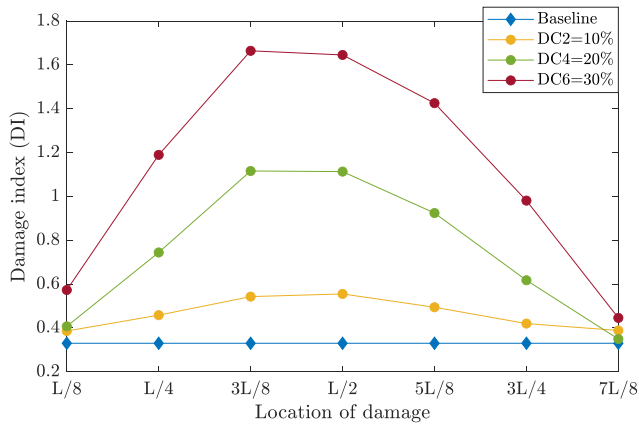


Fig. 12. Effect on damage index of different bridge damage locations (Scenario-1).

fluctuate because of operational effects and varying vehicle properties, but the distribution of errors tends to remain fixed. The characterization of that distribution is more precise when larger the number of events considered in its calculation. As shown in Fig. 11, the damage index fluctuates quite significantly for small fleet sizes. However, with increasing number of vehicles, variations in DI decrease. This shows that for a sufficiently large fleet size, the effect of operational conditions can be reduced. In this study a batch size of 250 vehicle-crossing events are deemed appropriate because it results in sufficiently small variations in DI.

5.1.2. Influence of location

In practical cases, the location of damage can be anywhere along the bridge's length and it has been often reported that it is difficult to detect damage close to the bridge's supports under realistic vehicle and operational conditions [7]. In vibration-based damage detection methods, the sensitivity to damage depends on the location. For instance, in the case of a damage close to the bridge support the variation in frequencies (mainly the lower frequencies) would be much less compared to the case with midspan damage. To detect the damage at different locations of the beam it is important to consider the full spectra of the signals. The proposed method considers time series responses, which include the complete frequency content, that enables the damage detection at different locations, to some extent.

To illustrate the robustness and accuracy of the proposed method, damage identification is conducted for different beam damage locations. The trained model for Scenario-1 is considered with batch sizes of 250 vehicle-crossing events. Fig. 12 shows the sensitivity of DI for damage cases at seven different locations along the beam. The variation in magnitude of the damage index for locations between $L/4$ and $3L/4$ is significant and comparable in order of magnitude to results at $L/2$. In case of locations closer to the supports ($L/8$ and $7L/8$) the magnitude of damage index for low damage severity cases is not distinguishable. However, if larger batch sizes were considered the robustness of the method increases. Then it would be possible to consistently distinguish smaller variations of DI due to damages near the supports.

5.1.3. Effect of vehicle speed

In vehicle assisted damage assessment, speed and mass of traversing vehicle is critical in the presence of road surface. Previously published studies [7,27] have shown that vehicles with relatively small masses travelling at high speeds cannot detect damage with sufficient accuracy. This is mainly due to the short duration of the vehicle signals, hence a poor resolution in the frequency domain, but also due to low levels of bridge excitation and the presence of road profile. In lightweight vehicles at high speeds, the bridge response component is masked by the dynamic effects induced by the road profile. Compared to that,

Table 3
Vehicle speed variability (in km/h).

Dataset name	Min.	Max.	Mean	SD
Dataset V1	25	40	36	7
Dataset V2	40	70	55	7
Dataset V3	70	120	90	7

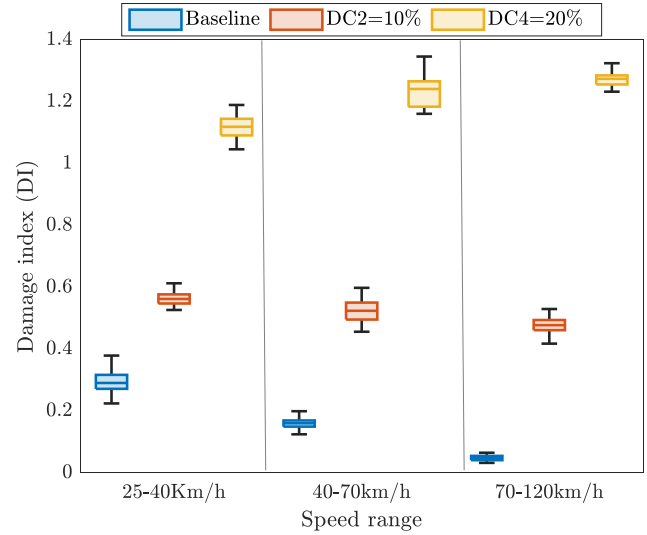


Fig. 13. Damage index performance comparison for different speed ranges.

heavyweight vehicles can sufficiently excite the bridge and are therefore considered more suitable for indirect bridge monitoring [34]. However, the amount of dynamic interaction between vehicle and bridge depends on the traversing speed. To study the effect of vehicle speed, three different speed ranges are studied for Scenario-1. New datasets are generated with the same properties as shown in Table A1 of the appendix except for the vehicle speeds. For each new dataset, the vehicle speeds are randomly sampled following normal distributions defined by the values provided in Table 3. Three DAE models are trained using tractor accelerations (\ddot{u}_{b1}), one for each new dataset. The trained models have tested against the baseline and two damage cases (DC2 and DC4). To consider the uncertainty in operational conditions (number of vehicle's, road profile etc) 20 randomly selected fleet size is considered from range of 200 to 400.

Fig. 13 compares the damage index distributions for three damage cases (baseline, DC2 and DC4) for three speed ranges (using datasets V1, V2 and V3). The comparison is done using a box plot representation, which shows the 25th and 75th percentile values in a box together with the median value and indicates the maximum and minimum results of the DI distribution. The results in all speed ranges allow for the clear distinction between healthy and damaged cases. It also shows that at lower speed the performance of the trained model is less accurate than at higher speeds. The magnitude of the damage index for the baseline condition shows that at lower speeds the feature space is not well generalised for the damage-sensitive features, compared to higher speeds. The physical interpretation on why damage detection is more robust at higher speed might be in the relative magnitudes between static and dynamic components of the bridge response. At lower speeds the bridge behaviour captured by the vehicle response is dominated by the quasi-static component. Only a small proportion of energy is present at the bridge frequencies, which are therefore hardly captured by the passing vehicle. It is found the proposed damage detection method performs well using responses of vehicles travelling at normal operational speeds.

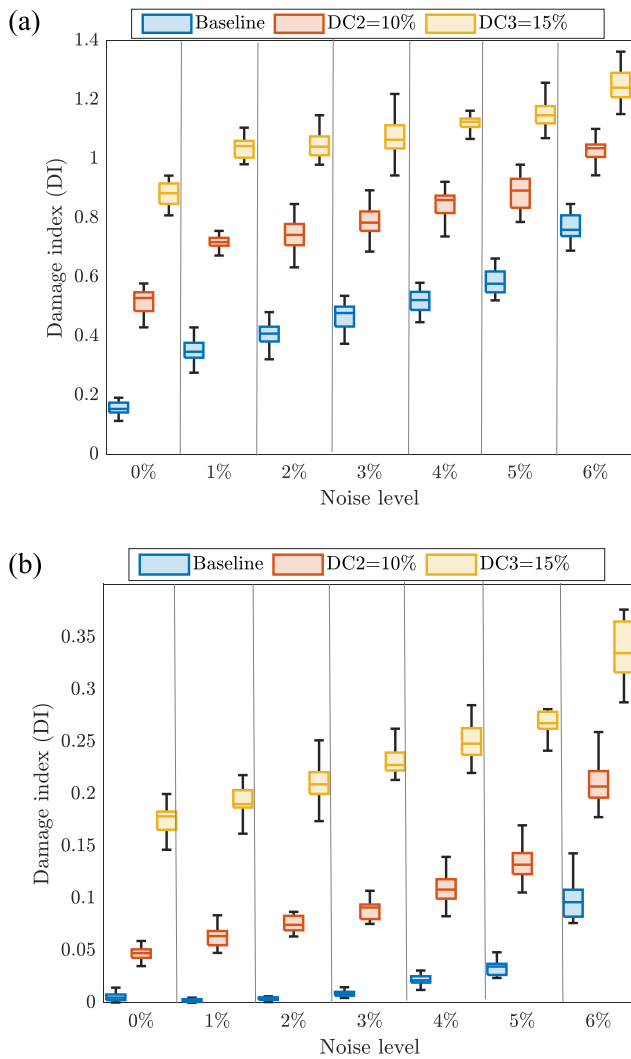


Fig. 14. Effect of measurement noise on the sensitivity of the damage index: (a) noise-free; (b) with noise.

5.1.4. Influence of measurement noise

This section presents the sensitivity and performance of the proposed damage detection method to measurement noise. In order to analyse the effect of noise, two separate datasets of 1000 vehicle-crossing events are considered. Dataset N1 was formed by noise-free samples and dataset N2 by adding normally distributed noise. Noise in acceleration response ($\ddot{u}_{b1,noise}$) is defined according to Eq. (14), for an equivalent noise level E_{level} .

$$\ddot{u}_{b1,noise} = \ddot{u}_{b1} + E_{level} \cdot N_{noise} \cdot \sigma(\ddot{u}_{b1}) \quad (14)$$

where, N_{noise} is a vector of standard normal distribution $N(0,1)$ and $\sigma(\ddot{u}_{b1})$ is the standard deviation of the measured response. In dataset N2, the noise level for each event is randomly sampled for $E_{level} N(2.5, 0.5)$ with value in the range $[0,5]$. Both datasets (N1 and N2) are trained using the architecture and hyperparameters discussed in Section 3.3. The trained models are then tested for three damage conditions (baseline, DC2 and DC3) by including a variations in noise levels E_{level} (noise-free or 0%, 1%, 2%, 3%, 4%, 5% and 6%). For each noise level to consider the statistical uncertainties because of operational variabilities 20 repeated simulation are computed with randomly selected fleet size from range of 200 to 400.

The noise sensitivity analysis of the proposed damage index (DI) for the two datasets is presented in Fig. 14. The results from both datasets clearly show that different levels of damages are separable even when

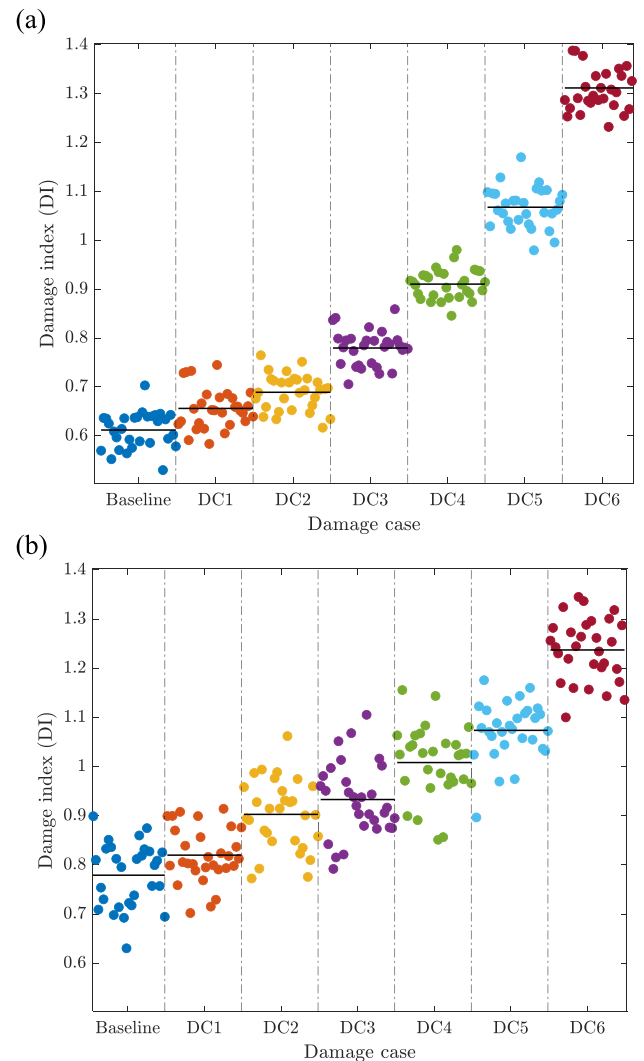


Fig. 15. Evolution of daily damage index (450 events/day) during progressive bridge condition change (every 30 days), for Scenario-2. Solid line indicates 30-day average value, using signals from: (a) tractor response (b) trailer response.

including large noise magnitudes in the signals. For dataset N1, when the model is trained with noise-free samples and tested with different noise levels, DI increases linearly with the increase in noise level (Fig. 14 (a)). It shows that the trained model starts overfitting with increases in noise and that variations in the noise level at baseline condition could be interpreted as damage. However, Fig. 14(b) shows the results of the same model but trained with dataset N2. The magnitude of DI for baseline condition remains approximately constant for a range of different noise levels compared to the noise-free model. The introduction of noise levels during the training process helped the DAE model to generalise the latent feature for healthy conditions under uncertainty. From these results, it can be said that the introduction of uncertainty in the form of measurement noise during model training results in a more stable performance for the baseline condition.

5.2. Damage detection for Scenario-2

This section discusses the damage assessment performance of the proposed method for Scenario-2, i.e. a more challenging scenario that uses a broader range of vehicle properties (as described in Section 3.2). For Scenario-2, separate DAE models are trained for both tractor and trailer responses of the vehicles. The trained models are tested for the damage cases discussed in Section 4, with the only difference that each

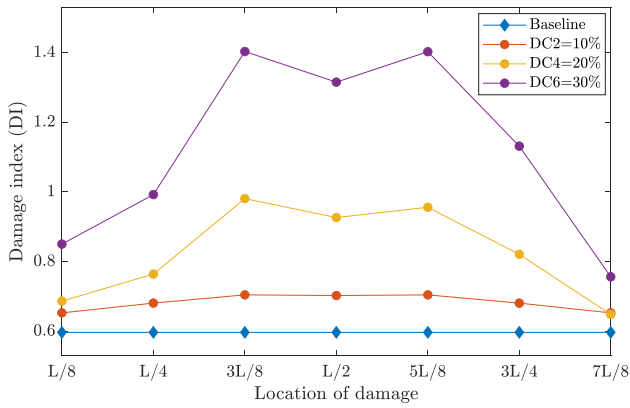


Fig. 16. Effect on damage index for different location of the bridge (Scenario-2).

case is simulated for the dataset of Scenario-2. Because of the inherent broader variability of the vehicle properties, the damage detection method benefits of larger sets of data. This is why 450 vehicles/day and intervals of 30 days are considered to illustrate the performance of the method, where the damage intensity is increased in 5% increments after 30 days. The results in terms of DI are shown in Fig. 15.

It is evident from Fig. 15, when compared to Scenario-1, that the daily variation in DI and the magnitude of DI for baseline condition are much higher. The trained models cannot fully generalise the latent space for damage sensitive features to accommodate the large variation in vehicles properties. However, the average value after 30 days is more robust and can easily distinguish different damage cases. Furthermore, as can be observed in Fig. 15(a), the daily fluctuation in DI when using the tractor signals is much less than for the model using the trailer signals Fig. 15(b). This significant difference between model results can be attributed to the inherent larger variability in properties of trailers. More in particular, trailers can vary considerably in dimensions, mass, and inertia properties, factors that have been accounted for during the random vehicle generation for Scenario-2. Therefore, the DAE model has more difficulties discerning damage sensitive features when using trailer responses, which in theory could be improved by increasing the number of events.

5.2.1. Influence of location

Finally, this section evaluates the sensitivity of the proposed method to damage location under the conditions of Scenario-2. Seven damage locations along the beam have been studied for different levels of damage severity. The trained model for tractor response is used with a batch size of 450 vehicles. Fig. 16 shows the damage index values for baseline condition and three damage cases (DC2, DC4, and DC 6). The magnitude of DI changes quite significantly for different locations. However, for a given damage location it is possible discern a healthy bridge (baseline) from a damaged one. The proposed method has clear damage detection capabilities, and since it is sensitive to damage location it could potentially be further developed to a damage localisation

Table 4

Bridge model properties and first three fundamental frequencies.

Symbol	Description	Value
L	Total span length (m)	89
E	Young's modulus (N/m ²)	$3.5 \cdot 10^{10}$
I	Second moment of area (m ⁴)	1.3427
A	Cross section area (m ²)	5.6180
ρ	Mass per unit length (kg/m)	2500
$k_{r, (1,2,3)}$	Rotational stiffness for supports (Nm/rad)	$4.5 \cdot 10^9$
$k_{v, (1,2,3)}$	Vertical stiffness for supports (N/m)	$3.5 \cdot 10^{10}$
ζ	Damping (%)	2
$f_{1,2,3} (model)$	First three calculated frequencies (Hz)	[4.91, 6.54, 13.45]
$f_{1,2,3} [62]$	First three measured frequencies (Hz)	[4.91, 6.53, 12.84]

tool.

In summary, it is shown that the proposed method can be used effectively for damage assessment using multiple vehicles responses. A DAE can be implemented that finds an adequate generalisation of the feature space together with damage sensitive features provided that enough data for training is available.

6. Performance validation on multi-span bridge

This section evaluates the performance of the proposed method simulating the behaviour of an existing multi-span continuous highway bridge. Furthermore, this study is extended to evaluate the effect of additional random traffic and its influence on the sensitivity of proposed damage index.

6.1. Voigt Drive I-5 bridge

The Voigt Drive I-5 bridge is located on the Eastern edge of the University of California, San Diego (UCSD). The four span reinforced concrete box girder structure is 89 m long and constitutes a typical large highway overpass. More details on the structure's properties, dimensions and configuration can be found in [62]. The bridge is modelled here as a multi-span continuous beam. The section properties of the beam are computed from the cross-section dimensions of the real bridge. The intermediate supports are modelled using vertical and rotational springs, as shown in Fig. 17. The values of the support springs are manually tuned to match the first three natural frequencies reported in [62].

Table 4 lists the final section and material properties and the first three natural frequencies of the model compared to the measured bridge frequencies.

In line with the studies performed in previous sections, the finite element model of the bridge is made of 0.5 m long elements (178 elements in total). A similar carpet road profile of class 'A' is included on bridge and vehicle's path, with a 100 m approach distance (as discussed in section 3.1.2). The coupled vehicle-bridge interaction model is solved using Eq. (12) to extract vehicle body acceleration responses.

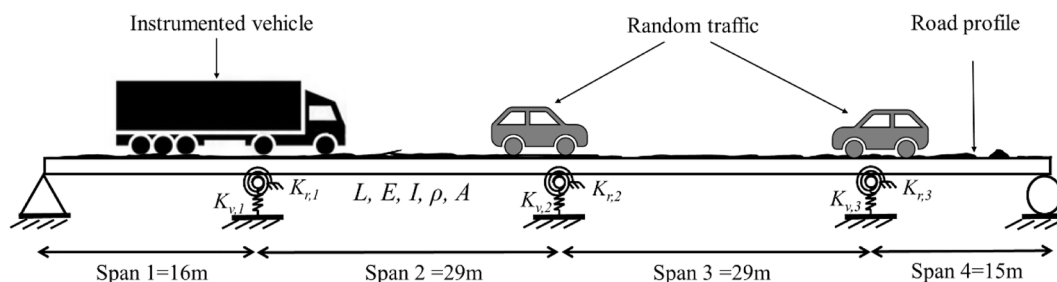


Fig. 17. Model of Voigt Drive I-5 bridge with instrumented vehicle and random traffic.

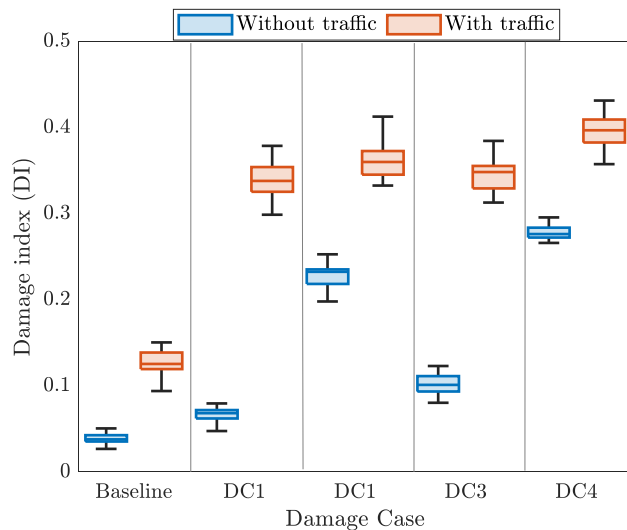


Fig. 18. Damage index performance comparison for multi-span bridge considering without traffic and with traffic.

6.2. Data generation and DAE training

To examine the sensitivity of the proposed damage index on the multi-span continuous bridge, two new scenarios are studied. One scenario consists of single 5-axle truck crossing events, which is subsequently referred to as ‘Without traffic’. On the other hand, the second new scenario includes additional random traffic on the bridge, which is termed ‘With traffic’. The dataset for both scenarios was generated by solving the vehicle-bridge interaction system presented in Section 3.1. For dataset generation the statistical variabilities of the 5-axle truck parameters remained the same as for Scenario-1 discussed in Section 3.2. However, for modelling the additional random traffic on the bridge for the ‘With traffic’ scenario, two 2-axle vehicles are included in the crossing event as shown in Fig. 19. These additional vehicles are assigned randomly sampled properties within a Monte Carlo simulation, allowing the vehicles to enter randomly from either left or right side of the bridge. Additional details on the 2-axle vehicle model and their statistical variabilities are provided in Table A2 in the Appendix.

For each new scenario batches, of 1000 vehicle events are created. Each dataset contains the vertical acceleration response from tractor (\ddot{u}_{b1}) and vehicle speed (v) of the traversing 5-axle truck. Each dataset is resampled from time-domain to space-domain to compute fixed length vectors with 1500 samples. A random sampled noise level of $E_{level} N(2.5, 0.5)$ with value in the range $[0, 5]$ is added to the datasets using Eq. (14). The DAE model with the same configuration and hyperparameters as discussed in Section 3.3 is used to train the model for a healthy bridge condition. The datasets are divided into 700 and 300 vehicle crossing events respectively for training and validation of the model.

To investigate the performance of the DAE and the sensitivity of the damage index, five new damage cases are defined. The type of damage and their location of each damage case are:

- Baseline: Healthy bridge
- DC1: 30% mid-span stiffness reduction on span 1 (at 8.5 m of the bridge)
- DC2: 30% mid-span stiffness reduction on span 2 (at 31 m of the bridge)
- DC3: 30% rotational stiffness ($k_{r,1}$) reduction at support 1
- DC4: 30% rotational stiffness ($k_{r,2}$) reduction at support 2

6.3. Damage detection for multi-span bridge

The five new damage cases are investigated for both new scenarios (‘Without traffic’ and ‘With traffic’) to assess the performance of the proposed method. For each damage case, 20 repeated simulation are computed with randomly selected fleet sizes ranging from 400 to 500 events. Then, as in Section 5, the distribution of the reconstruction loss is computed using Eq. (5) and the statistical parameters of fitted distributions are further used to compute the Damage index (DI) with Eq. (7).

Fig. 18 shows the damage sensitivity analysis for both new scenarios and the five new damage cases for the multi-span continuous bridge. The results suggest that in both scenarios, there is a clear distinction between baseline and damage cases. However, it is also evident from the figure that for the scenario with additional random traffic the severity comparison of different damage cases is relatively poor, compared to the scenario when no traffic is present on the bridge. This is because the trained model cannot fully generalise the latent space for damage sensitive features to accommodate the contribution of excitations from additional random traffic vehicles. However, broadly speaking this problem could be resolved by fine tuning the DAE model’s hyperparameters and increasing the training dataset. Nevertheless, aside from the performance degradation of the method when considering additional random traffic, the proposed method can clearly detect and quantify the severity of damages for the multi-span bridge model for all other cases. Therefore, the results suggest that the proposed method can be used for a wide range of structural configurations, making it a potentially useful approach for network-wide road bridge monitoring.

7. Practical consideration for real-life application

The method proposed in this paper may be useful to monitor bridges and assess their condition. The method relies on the fact that local damage, resulting in local bending stiffness reductions, directly affect the modal properties of the bridge. These variations can be identified from the vertical acceleration signals recorded by the on-board sensors of the traversing vehicles. However, it is impossible to identify these variations solely using signals from single events, due to the inherent fluctuations under operational conditions (e.g. vehicle velocity, road profile and signal noise). Instead, this study proposes the use of signals from a fleet of vehicles to capture the variations in bridge behaviour. The collected signals from multiple vehicles could then be used to extract the bridge dynamic features using DAE.

However, there exist multiple challenges for the practical implementation of the proposed method, including signal collection and synchronization, variable vehicle speed, threshold definition and other loads (wind, earthquake, temperature). Each of these challenges could potentially be adequately addressed by fully utilizing existing technologies.

Arguably, the main challenge to apply the proposed method is the collection of the necessary signals and related crossing event information from passing vehicles. However, this is gradually becoming a real possibility considering the current trends in the transport industry. Modern trucks are getting an increasing number of built-in sensors, which could include (if not already) also sensors measuring the vertical acceleration of the tractor. While entry and exit times of the vehicle on the bridge can be determined via global positioning systems. Furthermore, many truck vendors offer also comprehensive fleet management system solutions that could seamlessly accommodate the gathered information. In turn, this information can be used to devise correction measures on operational conditions such as variable vehicle speed or individual truck mechanical properties. In such a near future scenario, a fleet of transport trucks that regularly roam the road network would provide a reliable and abundant source of information to put the proposed idea into practice.

On the other hand, bridges are subjected not only to traffic loading but also to other types of actions. It is generally known that ambient

Table A1
5-axle truck model parameters.

5-Axle-truck Parameters	Scenario-1				Scenario-2			
	Min.	Max.	Mean	SD	Min.	Max.	Mean	SD
Mass (kg)								
Tractor body m_{b1}	2800	3400	3100	80	2500	4000	3200	250
Trailer body m_{b2}	15,000	25,000	20,000	1000	10,000	40,000	25,000	4500
Tractor axles m_{u1}, m_{u2}	500	1000	750	30	300	1000	600	100
Trailer axles m_{u3}, m_{u4}, m_{u5}	800	1400	1100	50	600	1600	1100	100
Moment of inertia (kg·m²)								
Tractor body I_{b1}	4250	5500	4875	50	4000	5800	4900	150
Trailer body I_{b2}	112,000	135,000	123,000	2500	106,000	140,000	123,000	6000
Viscous damping (N·s/m)								
Front suspensions C_{s1}, C_{s2}	$1.0 \cdot 10^4$	$8.0 \cdot 10^4$	$4.0 \cdot 10^4$	$0.5 \cdot 10^4$	$1 \cdot 10^4$	$12 \cdot 10^4$	$6 \cdot 10^4$	$2 \cdot 10^4$
Rear suspensions C_{s3}, C_{s4}, C_{s5}	$2 \cdot 10^5$	$16 \cdot 10^5$	$8 \cdot 10^4$	$1 \cdot 10^4$	$2 \cdot 10^4$	$24 \cdot 10^4$	$12 \cdot 10^4$	$4 \cdot 10^4$
Spring stiffness (N/m)								
Front suspensions K_{s1}, K_{s2}	$4.0 \cdot 10^6$	$8.0 \cdot 10^6$	$6.0 \cdot 10^6$	$0.5 \cdot 10^6$	$1 \cdot 10^6$	$12 \cdot 10^6$	$6 \cdot 10^6$	$1 \cdot 10^6$
Rear suspensions K_{s3}, K_{s4}, K_{s5}	$5.0 \cdot 10^6$	$15 \cdot 10^6$	$10 \cdot 10^6$	$0.5 \cdot 10^6$	$2.5 \cdot 10^6$	$15.0 \cdot 10^6$	$10.0 \cdot 10^6$	$2.0 \cdot 10^6$
Front tyre K_{t1}, K_{t2}	$1.25 \cdot 10^6$	$2.25 \cdot 10^6$	$1.75 \cdot 10^6$	$0.20 \cdot 10^6$	$1.0 \cdot 10^6$	$4.0 \cdot 10^6$	$2.0 \cdot 10^6$	$0.7 \cdot 10^6$
Rear tyre K_{t3}, K_{t4}, K_{t5}	$2.75 \cdot 10^6$	$4.75 \cdot 10^6$	$3.50 \cdot 10^6$	$0.20 \cdot 10^6$	$2.0 \cdot 10^6$	$8.0 \cdot 10^6$	$4.0 \cdot 10^6$	$1.0 \cdot 10^6$
Geometry (m)								
D_1	–	–	5	–	3.5	6.5	5.0	0.1
D_2	–	–	4	–	3.0	5.0	4.0	0.02
e_1	–	–	–1.09	–	–0.50	–1.20	–0.80	–0.01
e_2	–	–	3.5	–	3.00	4.00	3.50	0.05
e_3	–	–	1.2	–	–	–	1.2	–
e_4	–	–	2.2	–	–	–	2.2	–
e_5	–	–	3.2	–	–	–	3.2	–
Velocity (km/h)								
Velocity v	36	60	40	5	36	60	40	8

temperature fluctuations produce variations in the modal properties of bridges. Also, wind loading can be an important source of dynamic excitation, particularly on longer bridges. These effects could be compensated using dedicated sensors on the bridge to monitor these loads or utilizing the information available from nearby weather stations. In case of seismic activity, the duration of this exceptional load is very short. Any vehicle crossing event during earthquake excitation could be discarded without affecting the overall performance of the proposed method. However, if some damage occurs as result of an earthquake, the proposed method could be used to detect that damage.

Moreover, to implement a successful structural health monitoring system based on the proposed method, it is required to identify adequate thresholds for the damage index. The system has to identify potential damage occurrences while minimizing the number of false alarms. This challenge can be tackled using statistical techniques on the continuous stream of calculated damage indicators from each individual event. Over time, the study of statistical moments (mean and standard deviations) would provide indications of normal damage index values under operational conditions. Then large deviations on the damage index would indicate significant variations in the structural behaviour that could be attributed to a possible damage.

8. Conclusion

This study proposed a damage assessment technique based on deep learning and a statistical distribution-based damage index. The suggested SHM method uses the acceleration responses from multiple traversing vehicles over the target bridge. The major challenge in damage detection using the response from several different vehicles is to generalise the relationship between vehicle responses and bridge dynamics. To address this issue, this paper used deep autoencoders (DAE) architecture, considering multiple convolutional layers and LSTM layers

for dimensionality reduction. The DAE is trained for healthy (or existing) bridge conditions, which constructs a feature space that is sensitive to bridge dynamics and robust enough against measurement noise and operational conditions. Moreover, the errors between measured and reconstructed signals are characterized by distributions that are sensitive to bridge damage. The damage index based on the KL divergence of these distributions can be used for damage detection and severity quantification.

The proposed method's effectiveness is evaluated numerically with a 5-axle truck vehicle model traversing a simply supported bridge and multi-span continuous bridge. Two scenarios are considered based on the level of variability in vehicle properties and operational conditions for simply supported beam model. Similarly, for multi-span bridge model, effect of random traffic is also considered. The results show that the outlined method is able to detect damage successfully, providing robust results under operational conditions (road profile, vehicle properties variability and measurement noise). In conclusion, the proposed method has potential to become a practical tool as it removes the need of specialised vehicles for long-term bridge monitoring. Additionally, the proposed method can easily be integrated with an intelligent transport network and can be used as a cost-effective solution for bridge health monitoring.

CRediT authorship contribution statement

Muhammad Zohaib Sarwar: Conceptualization, Methodology, Software, Formal analysis, Writing – original draft. **Daniel Cantero:** Conceptualization, Supervision, Software, Writing – review & editing.

Declaration of Competing Interest

The authors declare that they have no known competing financial

Table A2
2-axle vehicle model parameters.

2-Axle-vehicle Parameters	'With traffic' scenario			
	Min.	Max.	Mean	SD
Mass (kg)				
Body mass m_b	5000	16,000	10,500	500
Tractor axles m_{s1}, m_{s2}	600	1200	900	100
Moment of inertia (kg·m²)				
Body I_b	45,000	65,000	53,651	2000
Viscous damping (N·s/m)				
Front suspensions C_{s1}, C_{s2}	$0.5 \cdot 10^4$	$1.5 \cdot 10^4$	$1.0 \cdot 10^4$	$0.2 \cdot 10^4$
Spring stiffness (N/m)				
Front suspensions K_{s1}, K_{s2}	$4.0 \cdot 10^6$	$8.0 \cdot 10^6$	$6.0 \cdot 10^6$	$0.5 \cdot 10^6$
Front tyre K_{t1}, K_{t2}	$1.25 \cdot 10^6$	$2.25 \cdot 10^6$	$1.75 \cdot 10^6$	$0.20 \cdot 10^6$
Axle spacing (m)				
e_1	4	9	–	–
Velocity (km/h)				
Velocity v	40	70	55	5

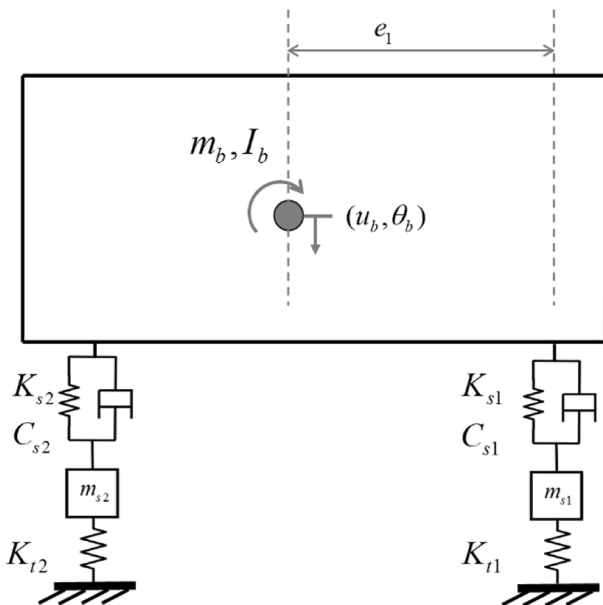


Fig. 19. 2-axle vehicle model.

interests or personal relationships that could have appeared to influence the work reported in this paper.

Appendix

Table A1 provides the model parameters with their statistical variability for simulation of 5-axle truck as shown in Fig. 3. Monte Carlo simulation used the statistical variability of the parameter to generate the dataset for two scenarios. Table A2 provides the model parameters with their statistical variability of 2-axle vehicles as shown in Fig. 19, which are used in the 'With traffic' scenario in Section 6

References

- Jang S, Jo H, Cho S, Mechitov K, Rice JA, Sim S-H, et al. Structural health monitoring of a cable-stayed bridge using smart sensor technology: deployment and evaluation. *Smart Struct Syst* 2010;6:439–59. <https://doi.org/10.12989/sss.2010.6.5.439>.
- Spencer BF, Ruiz-Sandoval ME, Kurata N. Smart sensing technology: opportunities and challenges. *Struct Control Health Monit* 2004;11(4):349–68. <https://doi.org/10.1002/stc.48>.
- Spencer BF, Park J-W, Mechitov KA, Jo H, Agha G. Next Generation Wireless Smart Sensors Toward Sustainable Civil Infrastructure. *Proc Eng* 2017;171:5–13. <https://doi.org/10.1016/j.proeng.2017.01.304>.
- An Y, Chatzi E, Sim S-H, Laflamme S, Blachowski B, Ou J. Recent progress and future trends on damage identification methods for bridge structures. *Struct Control Health Monitoring* 2019;26(10). <https://doi.org/10.1002/stc.2416>.
- Casas JR, Moughy JJ. Bridge Damage Detection Based on Vibration Data: Past and New Developments. *Front Built Environ* 2017;3. <https://doi.org/10.3389/fbuil.2017.00004>.
- Çelebi M. Real-Time Seismic Monitoring of the New Cape Girardeau Bridge and Preliminary Analyses of Recorded Data: An Overview. *Earthquake Spectra* 2006;22(3):609–30. <https://doi.org/10.1193/1.2219107>.
- Yang YB, Wang Z-L, Shi K, Xu H, Wu YT. State-of-the-Art of Vehicle-Based Methods for Detecting Various Properties of Highway Bridges and Railway Tracks. *Int J Str Stab Dyn* 2020;20(13):2041004. <https://doi.org/10.1142/S021945420410047>.
- Yang Y-B, Lin CW, Yau JD. Extracting bridge frequencies from the dynamic response of a passing vehicle. *J Sound Vib* 2004;272(3-5):471–93. [https://doi.org/10.1016/S0022-460X\(03\)00378-X](https://doi.org/10.1016/S0022-460X(03)00378-X).
- Malekjafarian A, McGetrick PJ, O'Brien EJ. A Review of Indirect Bridge Monitoring Using Passing Vehicles. *Shock Vib* 2015;2015:1–16. <https://doi.org/10.1155/2015/286139>.
- Matarazzo TJ, Kondor D, Santi P, Milardo S, Eshkevari SS, Pakzad SN, et al. Crowdsourcing Bridge Vital Signs with Smartphone Vehicle Trips. *ArXiv: 201007026 [Physics]*; 2020.
- Lin CW, Yang YB. Use of a passing vehicle to scan the fundamental bridge frequencies: An experimental verification. *Eng Struct* 2005;27(13):1865–78. <https://doi.org/10.1016/j.engstruct.2005.06.016>.
- Yang YB, Chang KC. Extracting the bridge frequencies indirectly from a passing vehicle: Parametric study. *Eng Struct* 2009;31(10):2448–59. <https://doi.org/10.1016/j.engstruct.2009.06.001>.
- Zhu L, Malekjafarian A. On the Use of Ensemble Empirical Mode Decomposition for the Identification of Bridge Frequency from the Responses Measured in a Passing Vehicle. *Infrastructures* 2019;4:32. <https://doi.org/10.3390/infrastructures4020032>.
- O'Brien EJ, Malekjafarian A, González A. Application of empirical mode decomposition to drive-by bridge damage detection. *Eur J Mech A Solids* 2017;61: 151–63. <https://doi.org/10.1016/j.euromechsol.2016.09.009>.
- Kildashti K, Makki Alamdari M, Kim CW, Gao W, Samali B. Drive-by-bridge inspection for damage identification in a cable-stayed bridge: Numerical investigations. *Eng Struct* 2020;223:110891. <https://doi.org/10.1016/j.engstruct.2020.110891>.
- Zhu XQ, Law SS. Wavelet-based crack identification of bridge beam from operational deflection time history. *Int J Solids Struct* 2006;43(7-8):2299–317. <https://doi.org/10.1016/j.ijsolstr.2005.07.024>.
- O'Brien EJ, Malekjafarian A. A mode shape-based damage detection approach using laser measurement from a vehicle crossing a simply supported bridge. *Struct Control Health Monitoring* 2016;23(10):1273–86. <https://doi.org/10.1002/stc.1841>.
- Yang YB, Li YC, Chang KC. Constructing the mode shapes of a bridge from a passing vehicle: a theoretical study. *Smart Struct Syst* 2014;13:797–819. <https://doi.org/10.12989/sss.2014.13.5.797>.
- Malekjafarian A, O'Brien EJ. On the use of a passing vehicle for the estimation of bridge mode shapes. *J Sound Vib* 2017;397:77–91. <https://doi.org/10.1016/j.jsv.2017.02.051>.
- Sadeghi Eshkevari S, Matarazzo TJ, Pakzad SN. Bridge modal identification using acceleration measurements within moving vehicles. *Mech Syst Sig Process* 2020; 141:106733. <https://doi.org/10.1016/j.ymsp.2020.106733>.
- O'Brien EJ, McGetrick PJ, Gonzalez A. A drive-by inspection system via vehicle moving force identification. *Smart Struct Syst* 2014;13:821–48. <https://doi.org/10.12989/sss.2014.13.5.821>.
- Quirke P, Bowe C, O'Brien EJ, Cantero D, Antolin P, Goicolea JM. Railway bridge damage detection using vehicle-based inertial measurements and apparent profile. *Eng Struct* 2017;153:421–42. <https://doi.org/10.1016/j.engstruct.2017.10.023>.
- Zhu XQ, Law SS, Huang L, Zhu SY. Damage identification of supporting structures with a moving sensory system. *J Sound Vib* 2018;415:111–27. <https://doi.org/10.1016/j.jsv.2017.11.032>.
- Liu J, Bergés M, Bielak J, Garrett JH, Kovačević J, Noh HY. A damage localization and quantification algorithm for indirect structural health monitoring of bridges using multi-task learning. *AIP Conf Proc* 2019;2102:090003. <https://doi.org/10.1063/1.5099821>.
- Mei Q, Gül M, Boay M. Indirect health monitoring of bridges using Mel-frequency cepstral coefficients and principal component analysis. *Mech Syst Sig Process* 2019; 119:523–46. <https://doi.org/10.1016/j.ymsp.2018.10.006>.
- Malekjafarian A, Golpayegani F, Moloney C, Clarke S. A Machine Learning Approach to Bridge-Damage Detection Using Responses Measured on a Passing Vehicle. *Sensors (Basel)* 2019;19. <https://doi.org/10.3390/s19184035>.
- Zhang B, Qian Y, Wu Y, Yang YB. An effective means for damage detection of bridges using the contact-point response of a moving test vehicle. *J Sound Vib* 2018;419:158–72. <https://doi.org/10.1016/j.jsv.2018.01.015>.
- Fitzgerald PC, Malekjafarian A, Cantero D, O'Brien EJ, Prendergast LJ. Drive-by scour monitoring of railway bridges using a wavelet-based approach. *Eng Struct* 2019;191:1–11. <https://doi.org/10.1016/j.engstruct.2019.04.046>.

- [29] McGettrick PJ, Kim C-W, González A, Brien EJO. Experimental validation of a drive-by stiffness identification method for bridge monitoring. *Struct Health Monitoring* 2015;14(4):317–31. <https://doi.org/10.1177/1475921715578314>.
- [30] McGettrick PJ, Kim CW. A Parametric Study of a Drive by Bridge Inspection System Based on the Morlet Wavelet. *Key Eng Mater* 2013;569–570:262–9. <https://doi.org/10.4028/www.scientific.net/KEM.569-570.262>.
- [31] Hester D, González A. A discussion on the merits and limitations of using drive-by monitoring to detect localised damage in a bridge. *Mech Syst Sig Process* 2017;90:234–53. <https://doi.org/10.1016/j.ymssp.2016.12.012>.
- [32] Lederman G, Wang Z, Bielak J, Noh HY, Garrett J, Chen S, et al. Damage quantification and localization algorithms for indirect SHM of bridges. 2014. <https://doi.org/10.1201/B17063-93>.
- [33] Liu J, Chen S, Bergés M, Bielak J, Garrett JH, Kovačević J, et al. Diagnosis algorithms for indirect structural health monitoring of a bridge model via dimensionality reduction. *Mech Syst Sig Process* 2020;136:106454. <https://doi.org/10.1016/j.ymssp.2019.106454>.
- [34] Miyamoto A, Yabe A, Brühwiler E. A Vehicle-based Health Monitoring System for Short and Medium Span Bridges and Damage Detection Sensitivity. *Proc Eng* 2017;199:1955–63. <https://doi.org/10.1016/j.proeng.2017.09.299>.
- [35] Locke W, Sybrandt J, Redmond L, Safro I, Atamturktur S. Using drive-by health monitoring to detect bridge damage considering environmental and operational effects. *J Sound Vib* 2020;468:115088. <https://doi.org/10.1016/j.jsv.2019.115088>.
- [36] Relationship with the ITS Action Plan and ITS Directive | FRAME ARCHITECTURE n.d. <https://frame-online.eu/frame-architecture/detailed-information/relationshi-p-with-the-its-action-plan-and-its-directive> (accessed January 3, 2021).
- [37] Malekian R, Moloisane NR, Nair L, Maharaj BT, Chude-Onkonkwo UAK. Design and Implementation of a Wireless OBD II Fleet Management System. *IEEE Sens J* 2017;17(4):1154–64. <https://doi.org/10.1109/JSEN.2016.2631542>.
- [38] Billhardt H, Fernandez A, Lemus L, Lujak M, Osman N, Ossowski S, et al. Dynamic Coordination in Fleet Management Systems: Toward Smart Cyber Fleets. *IEEE Intell Syst* 2014;29(3):70–6. <https://doi.org/10.1109/MIS.2014.41>.
- [39] Hinton GE, Salakhutdinov RR. Reducing the Dimensionality of Data with Neural Networks. *Science* 2006;313:504–7. <https://doi.org/10.1126/science.1127647>.
- [40] Arel I, Rose DC, Karnowski TP. Deep Machine Learning - A New Frontier in Artificial Intelligence Research [Research Frontier]. *IEEE Comput Intell Mag* 2010;5(4):13–8. <https://doi.org/10.1109/MCI.2010.938364>.
- [41] Schmidhuber J. Deep learning in neural networks: An overview. *Neural Networks* 2015;61:85–117. <https://doi.org/10.1016/j.neunet.2014.09.003>.
- [42] Avci O, Abdeljaber O, Kiranyaz S, Hussein M, Gabbouj M, Inman DJ. A review of vibration-based damage detection in civil structures: From traditional methods to Machine Learning and Deep Learning applications. *Mech Syst Sig Process* 2021;147:107077. <https://doi.org/10.1016/j.ymssp.2020.107077>.
- [43] Abdeljaber O, Avci O, Kiranyaz S, Gabbouj M, Inman DJ. Real-time vibration-based structural damage detection using one-dimensional convolutional neural networks. *J Sound Vib* 2017;388:154–70. <https://doi.org/10.1016/j.jsv.2016.10.043>.
- [44] Ni F, Zhang J, Noori MN. Deep learning for data anomaly detection and data compression of a long-span suspension bridge. *Comput-Aided Civ Infrastruct Eng* 2020;35(7):685–700. <https://doi.org/10.1111/mice.v35.710.1111/mice.12528>.
- [45] Zhang Y, Miyamori Y, Mikami S, Saito T. Vibration-based structural state identification by a 1-dimensional convolutional neural network. *Comput-Aided Civ Infrastruct Eng* 2019;34(9):822–39. <https://doi.org/10.1111/mice.v34.910.1111/mice.12447>.
- [46] Wang Z, Cha Y-J. Unsupervised deep learning approach using a deep auto-encoder with an one-class support vector machine to detect structural damage. 1475921720934051 *Struct Health Monitoring* 2020. <https://doi.org/10.1177/1475921720934051>.
- [47] Shang Z, Sun L, Xia Y, Zhang W. Vibration-based damage detection for bridges by deep convolutional denoising autoencoder. *Struct Health Monitoring* 2021;20(4):1880–903. <https://doi.org/10.1177/1475921720942836>.
- [48] Sony S, Dunphy K, Sadhu A, Capretz M. A systematic review of convolutional neural network-based structural condition assessment techniques. *Eng Struct* 2021;226:111347. <https://doi.org/10.1016/j.engstruct.2020.111347>.
- [49] Zhang Q, Barri K, Babanajad SK, Alavi AH. Real-Time Detection of Cracks on Concrete Bridge Decks Using Deep Learning in the Frequency Domain. *Engineering* 2020. <https://doi.org/10.1016/j.eng.2020.07.026>.
- [50] Liu T, Li Z, Yu C, Qin Y. NIRS feature extraction based on deep auto-encoder neural network. *Infrared Phys Technol* 2017;87:124–8. <https://doi.org/10.1016/j.infrared.2017.07.015>.
- [51] Pascanu R, Mikolov T, Bengio Y. On the difficulty of training recurrent neural networks. *International Conference on Machine Learning*, PMLR 2013:1310–8.
- [52] Hochreiter S, Schmidhuber J. Long Short-Term Memory. *Neural Comput* 1997;9(8):1735–80. <https://doi.org/10.1162/neco.1997.9.8.1735>.
- [53] Joyce JM. Kullback-Leibler Divergence. In: Lovric M, editor. *International Encyclopedia of Statistical Science*. Berlin, Heidelberg: Springer; 2011. p. 720–2. https://doi.org/10.1007/978-3-642-04898-2_327.
- [54] Mei Q, Gül M. A crowdsourcing-based methodology using smartphones for bridge health monitoring. *Struct Health Monitoring* 2019;18(5-6):1602–19. <https://doi.org/10.1177/1475921718815457>.
- [55] Cantero D, O'Brien EJ, González A. Modelling the vehicle in vehicle—infrastructure dynamic interaction studies. *Proc Inst Mech Eng, Part K: J Multi-Body Dyn* 2010;224:243–8. <https://doi.org/10.1243/14644193JMBD228>.
- [56] Harris NK, OBrien EJ, González A. Reduction of bridge dynamic amplification through adjustment of vehicle suspension damping. *J Sound Vib* 2007;302(3):471–85. <https://doi.org/10.1016/j.jsv.2006.11.020>.
- [57] González A, Mohammed O. Dynamic Amplification Factor of Continuous versus Simply Supported Bridges Due to the Action of a Moving Vehicle. *Infrastructures* 2018;3:12. <https://doi.org/10.3390/infrastructures3020012>.
- [58] González A, Cantero D, OBrien EJ. Dynamic increment for shear force due to heavy vehicles crossing a highway bridge. *Comput Struct* 2011;89:2261–72. <https://doi.org/10.1016/j.compstruc.2011.08.009>.
- [59] Zhou X-Y, Treacy M, Schmidt F, Brühwiler E, Toutlemonde F, Jacob B. Effect on Bridge Load Effects of Vehicle Transverse In-Lane Position: A Case Study. *J Bridge Eng* 2015;20(12):04015020. [https://doi.org/10.1061/\(ASCE\)BE.1943-5592.0000763](https://doi.org/10.1061/(ASCE)BE.1943-5592.0000763).
- [60] Cantero D, González A, OBrien EJ. Comparison of Bridge Dynamic Amplifications Due to Articulated 5-Axle Trucks and Large Cranes. *Baltic J Road Bridge Eng* 2011;6:39–47. <https://doi.org/10.3846/bjrbe.2011.06>.
- [61] van der Maaten L, Hinton G. Visualizing Data using t-SNE. *J Machine Learning Res* 2008;9:2579–605.
- [62] Fraser M, Elgamal A, He X, Conte JP. Sensor Network for Structural Health Monitoring of a Highway Bridge. *J Comput Civil Eng* 2010;24(1):11–24. [https://doi.org/10.1061/\(ASCE\)CP.1943-5487.0000005](https://doi.org/10.1061/(ASCE)CP.1943-5487.0000005).